Wang *et al. Biochar* (2026) 8:72
https://doi.org/10.1007/s42773-026-00589-w

Biochar

ORIGINAL RESEARCH Open Access

Increased soil salinization slows biochar aging and limits microbial colonization

Ruoyu Wang[1], Hongqiang Li[1], Naqi Cui[2], Chong Tang[1], Xiangping Wang[1], Wenping Xie[1] and Rongjiang Yao[1*]

Abstract

Biochar is widely recognized as a green and sustainable amendment for saline-alkali soils. However, the aging process can alter its properties and compromise its long-term effectiveness in improving soil quality. Despite its significance, limited information is available on biochar aging in saline soils. This study investigated the mechanisms by which soil salinization influences biochar aging and microbial colonization characteristics. Biochar samples collected from agricultural fields with different salinity levels were subjected to repeated wet–dry cycles simulating approximately 8 years of natural aging and analyzed for changes in chemical and microbial properties. The results revealed that increased soil salinization slowed the aging process of biochar. Biochar aged in high-salinity soils retained significantly higher total carbon, aromaticity, and surface C–C/C = C carbon contents than those in low-salinity soils, whereas its total oxygen content, degree of oxidation, and surface C–O content were markedly lower. In the final cycle, the O/C ratio of biochar aged in high-salinity soil was 9.82% lower than that in low-salinity soil. Soil salinity also suppressed microbial community activity and diversity in the biochar, particularly fungi, likely contributing to the retardation of biochar aging. In addition, the barrier formed by soil mineral salts on the biochar surface further slowed the aging process. Additionally, temporal analysis revealed that over time, the oxidability of biochar increased due to the loss of labile carbon and the mineralization of organic matter, whereas the total carbon content decreased by approximately 20%. These findings enhance our understanding of biochar aging in saline soils and provide insights into its long-term environmental performance as a sustainable amendment.

Highlights

- Increased soil salinization slowed the aging process of biochar.
- Oxidability of aged biochar decreased with increasing salinization.
- C–C/C=C content and aromaticity of aged biochar increased with increasing salinization.
- Biochar in highly saline soils showed reduced microbial activity and diversity.
- Microbial activity may influence biochar aging in saline soils.

Keywords Biochar aging, Saline soil, Chemical properties, Microbial colonization, Wet–dry cycles

*Correspondence:
Rongjiang Yao
rjyao@issas.ac.cn
Full list of author information is available at the end of the article

Springer

Graphical Abstract

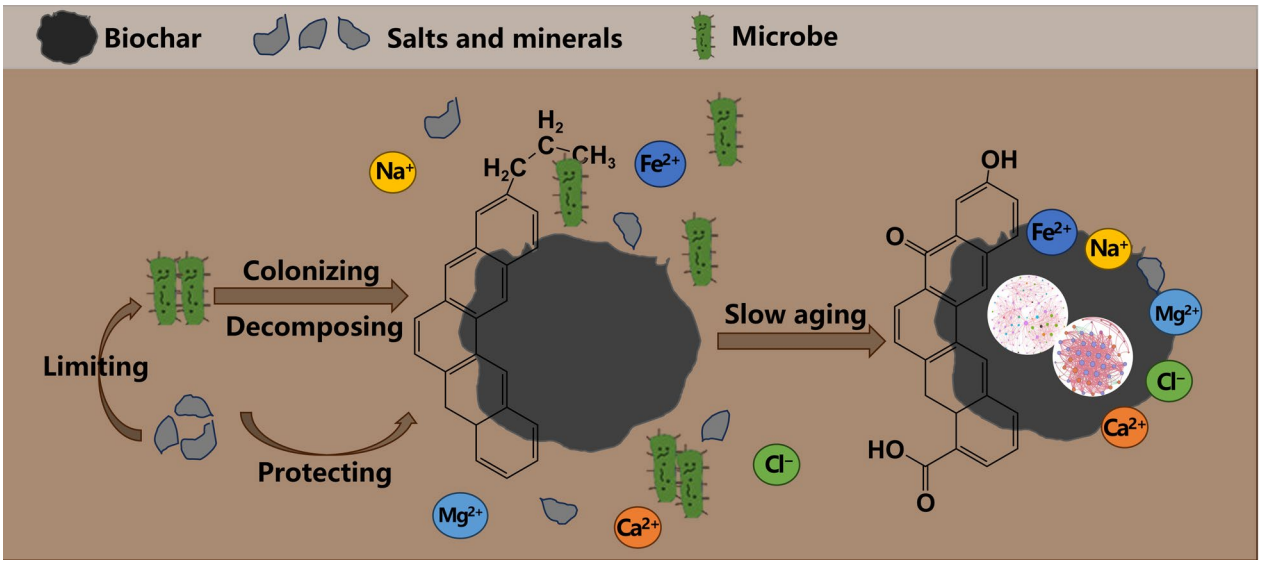

1 Introduction

Soil salinization is a critical global issue that contributes to land degradation and adversely affects certain soil properties, such as increased salt content, low hydraulic conductivity, nutrient deficiencies, and poor aeration, all of which severely constrain soil productivity (Xie et al. 2020; Li et al. 2023). In recent years, biochar has gained widespread application as a soil amendment for saline soils (Jin et al. 2024; Wang et al. 2023). It significantly enhances the physicochemical properties of salt-stressed soils and improves soil fertility (Piao et al. 2023; Wang et al. 2025). Biochar, produced by pyrolysis of biomass feedstocks under oxygen-limited, high-temperature conditions, is characterized by low production cost, a large specific surface area (SSA), strong adsorption capacity, and high stability (Luo et al. 2023). Over time, biochar in soil undergoes a natural aging process that alters its properties and environmental functions (Yi et al. 2020; Long et al. 2024). Natural factors such as rainfall, freezing and thawing, atmospheric oxidation, and soil biological activity contribute to the mechanical fragmentation, surface oxidation, and biodegradation of biochar, thereby inducing notable changes in its properties (Zhao et al. 2015; Silber et al. 2010; Yang et al. 2016; Quilliam et al. 2013). The intrinsic properties and temporal changes of biochar influence its ecological functions, including soil improvement and nutrient cycling (Li et al. 2016). For instance, studies have indicated that the long-term release of dissolved organic carbon (DOC) from aging biochar can enhance soil pollutant adsorption by opening biochar pores (Wang et al. 2022). Additionally, the formation of oxygen-containing functional groups during aging can reduce nitrogen leaching and improve nitrogen use efficiency (Esfandbod et al. 2017; Mia et al. 2017a, b). Therefore, a thorough understanding of biochar aging and its impact is essential for optimizing its application in soil remediation and sustainable land management.

Recent studies have explored changes in biochar properties following natural aging in field soils or artificial aging over several years. These changes encompass physical properties (e.g., morphology, SSA, and porosity), chemical properties (e.g., pH, surface functional groups, elemental composition, aromaticity, and cation exchange capacity), and biological properties (e.g., microbial activity, community structure, and diversity) (Bandara et al. 2021; Ge et al. 2024; Wang et al. 2020). These alterations are influenced by multiple factors, including biochar type, soil characteristics, and aging method (Liu et al. 2022). Compared with fresh biochar, aged biochar typically exhibits structural disruption and mechanical disintegration, which are often associated with rainfall and freeze–thaw events (Rafiq et al. 2020). As biochar ages, its carbon content generally decreases, whereas its oxygen content increases, reflecting the dissolution of unstable carbon and the formation of oxygen-containing functional groups (Mia et al. 2017a, b). Biochar oxidation can occur abiotically or biotically. Over extended periods, microorganisms become extensively colonized within biochar (Quilliam et al. 2013), The higher the labile carbon content (e.g., aliphatic C compounds),

the more rapid the colonization (Luo et al. 2013). After biochar is added to soil, minerals can interact with it through adsorption reactions and attach onto its surface, enhancing long-term carbon sequestration. However, natural aging of biochar proceeds extremely slowly, with a half-life of up to 1,000 years (Spokas 2010), Consequently, most studies adopt artificial aging methods (e.g., wet–dry cycles, freeze–thaw cycles, chemical oxidation, or biological aging) to simulate natural aging and shorten the experimental duration (Li et al. 2019).

The aging effects and mechanisms of biochar require comprehensive and in-depth investigation to establish a theoretical foundation for its effective application as a sustainable soil amendment. However, the long-term behavior of biochar under saline stress remains poorly understood and requires further investigation. In particular, limited research has explored how biochar properties change under the influence of soil salinity and how microbial communities respond to biochar aging. Such investigations are crucial for evaluating the ecological functions of biochar and its long-term effectiveness in improving saline soils.

To address these knowledge gaps, this study aimed to investigate changes in the chemical and biological properties of biochar across different salinity levels and aging durations and to elucidate the underlying aging mechanisms. Soils with varying degrees of salinization were collected from natural farmlands to simulate realistic aging conditions. Biochar was subjected to artificial aging through multiple wet–dry cycles, followed by material characterization and high-throughput analysis of microbial communities. We proposed the following research hypotheses: (1) Biochar undergoes carbon loss and oxidative modification after long-term aging in saline soils. (2) The salinity gradient affects the rate of carbon decline in biochar. (3) Microbial colonization occurs in aged biochar and responds to the salinity gradient. These findings are expected to enhance the understanding of biochar–soil–microbe interactions under saline conditions and support the long-term application of biochar in saline agricultural fields.

2 Materials and methods

2.1 Soil sampling and biochar preparation

Saline farmland soil was collected from the 0–20 cm layer at the Tiaozini National Wetland Protection Park (32 °51′22.89″ N, 120 °56′17.08″ E) in Dongtai City, Yancheng City, Jiangsu Province (Zhu et al. 2020). This farmland, located approximately 1 km from the Yellow Sea, has a subtropical monsoon marine climate with an annual average temperature of 14.8 °C. Approximately 70% of the annual rainfall (1046.3 mm) occurs between May and September, with annual evaporation of approximately 1.4 times the rainfall. According to soil salinization classification criteria (Wang et al. 1993; Tang et al. 2025), three types of saline soils, including low-salinity (LS), moderate-salinity (MS), and high-salinity (HS), were collected from different locations within the same farmland, dried, ground, and passed through a 2 mm sieve. According to soil taxonomy, the samples were classified as loam. Fresh biochar (FB) was produced by pyrolyzing wheat straw at 400 °C in a muffle furnace and then ground to pass through a 0.038 mm sieve. Low-temperature biochar retains more labile carbon (e.g., dissolved organic carbon and hemicellulose), which can be more readily utilized by microorganisms, thereby stimulating microbial activity and improving the soil ecological environment (Li et al. 2020). The basic physical and chemical properties of the soil and biochar are listed in Table 1.

2.2 Biochar aging and extraction

The experiment consisted of 12 treatments (three salinity gradients × four aging cycles), each replicated three times. Previous field and laboratory experiments have demonstrated that a 2% application rate can effectively improve the physicochemical properties of saline soils (Manasa et al. 2020). Soil (1 kg) was thoroughly mixed with 20 g of fresh biochar (2% of soil weight) to form a biochar–soil mixture, which was placed in 36 culture bottles. The soil for each replicate was obtained from the same location. Each replicate was treated independently, with biochar and soil mixed separately in individual bottles. Ultrapure water was added to saturate the samples to ensure uniform water content, after which they were incubated at 25 °C for 24 h. The samples were then dried at 45 °C for 24 h to mimic natural conditions conducive to microbial survival (Liu et al. 2022; Yang et al. 2022; Cruz-Paredes et al. 2021). During incubation and drying, the bottles were randomly and unorderly placed in the incubator and oven. This process constituted one wet–dry cycle over two days. Destructive sampling was

Table 1 Basic properties of soil and biochar

	LS	MS	HS	FB
pH	8.72	8.76	8.84	10.06
EC (μS cm^{-1})	341.8	1162.5	1905.5	4091
TS (g kg^{-1})	1.85	3.91	5.77	152.93
TO (g kg^{-1})	32.16	35.97	30.11	9.39
OM (g kg^{-1})	8.88	9.88	11.97	296.38
TN (g kg^{-1})	0.76	0.78	0.72	8.19
TP (g kg^{-1})	0.45	0.45	0.62	5.44

TS total salt, *TO* total oxygen, *OM* organic matter, *TN* total nitrogen, *TP* total phosphorus

performed at the end of each aging cycle (days 20, 40, 60, and 80). According to data from the China Meteorological Administration, Dongtai in China experienced an average of 4.7 d per year, with precipitation exceeding 50 mm between 2013 and 2023. We assumed that precipitation exceeding 50 mm would initiate the wet aging process (Meng et al. 2020; Xu et al. 2018). Ten wet–dry cycles in this study were considered to represent approximately 2 years of environmental conditions in Dongtai, and 40 complete cycles in this study reflected the natural aging process of 8 years (Meng et al. 2020, 2022). To separate biochar from soil, the mixtures were suspended in pure water, stirred, and allowed to stand for 12 h. Biochar floated to the surface, whereas the soil settled at the bottom (Meiirkhanuly et al. 2020). The upper liquid was pumped and filtered to collect the black solids, which were then washed, centrifuged, and oven-dried at 45 °C to obtain the aged biochar. The biochar samples were designated as LB1–4, MB1–4, and HB1–4, corresponding to their salinity levels and aging cycles. The biochar-soil mixtures were labeled LS1–4, MS1–4, and HS1–4.

2.3 Biochar characterization

All fresh and aged biochar samples were analyzed using scanning electron microscopy (SEM, ZEISS Sigma 300, Germany) under consistent operational parameters. The crystal structure of the biochar was characterized by X-ray diffraction (XRD, Bruker D2 Phaser, Germany), scanned at a rate of 5° min^{-1} over a 2θ range of 10–80°. The XRD patterns were analyzed using Jade 6.5 software to identify mineral compositions. Surface functional groups were identified using a Fourier transform infrared spectrometer (FTIR, Thermo Fisher Scientific Nicolet iS20, USA) in the range of 500–4000 cm^{-1} at a resolution of 2 cm^{-1}. Elemental compositions (C, O, H, and N) were determined using an elemental analyzer (EA, Thermo Fisher Scientific Flash 2000, USA). The degree of oxidation was estimated from the O/C molar ratio, while the H/C molar ratio served as an indicator of aromaticity and carbonation levels. Surface elemental composition and chemical states were analyzed using X-ray photoelectron spectroscopy (XPS, Thermo Scientific ESCALAB 250Xi, USA), and data were processed using Thermo Avantage software for peak identification, fitting, and charge calibration. Additionally, X-ray fluorescence spectroscopy (XRF) was conducted using a SHIMADZU XRF-1800 (Japan).

2.4 Microbial diversity analysis

The microbial community structures of biochar and soil samples from aging cycle IV (LB4, MB4, HB4, LS4, MS4, and HS4) stored at −80 °C were analyzed using high-throughput sequencing and quantitative polymerase chain reaction (qPCR). The microbial communities of the background samples were also analyzed to eliminate the influence of intrinsic microorganisms. DNA was extracted using an E.Z.N.A™ Mag-Bind Soil DNA Kit (OMEGA). For microbial community diversity analysis, the 16S rRNA gene was amplified using primers 16S-F (GTGCCAGCMGCCGCGGTAA) and 16S-R (CCCCGY CAATTCMTTTRAGT), whereas the ITS rRNA gene was amplified using primers ITS-F (GCATCGATGAAG AACGCAGC) and ITS-R (TCCTCCGCTTATTGATAT GC). The Silva (v138.1_16s) database was employed for bacteria and the UNITE (v9.0_its) database for fungi, with the analysis conducted in QIIME2 (2019.4). Dada2 (ver1.1) was used for sequence analysis. Details of soil DNA extraction, sequencing, and data processing are provided in the Supplementary Materials.

2.5 Statistical analysis

Experimental data were presented as the mean ± standard deviation, and significant differences ($p < 0.05$) between the treatments were determined using ANOVA in SPSS 26, followed by Tukey's Honestly Significant Difference (HSD) test for post hoc multiple comparisons. To examine the reciprocal effects of soil salinity and aging time on biochar aging, multivariate ANOVA was performed, and results were visualized using OriginPro 2021. Correlation between biochar properties and soil salinity was analyzed using the linkET package in R software, whereas redundancy analysis (RDA) in CANOCO 5 was used to assess the relationship between the microbial community structure and biochar properties ($p < 0.05$). Ecological networks of bacterial and fungal communities were constructed based on Spearman's correlation coefficients ($r > 0.7$, $p < 0.05$). Network analysis and topological parameters were calculated using the igraph package in R (Table S4), and co-occurrence networks were visualized using Gephi. Additional details of microbial data analysis are provided in the Supplementary Materials.

3 Results

3.1 Variation in biochar morphology during aging

The surface morphologies of fresh and aged biochars are shown in Fig. 1. Fresh biochar exhibited a rough surface coated with inorganic salts and organic oils while retaining the original pore structure of the plant material (Fig. 1a–c). After the first aging cycle, the biochar surface became smoother (Fig. S1), with localized fragmentation occurring at weaker edges. As the aging cycles progressed, fragmentation intensified, leading to substantial structural damage and loss of integrity. Diverse physical aging phenomena were observed, including the formation of new pores (Fig. 1d), local surface rupture and fragmentation (Fig. 1e), pore structure erosion (Fig. 1f),

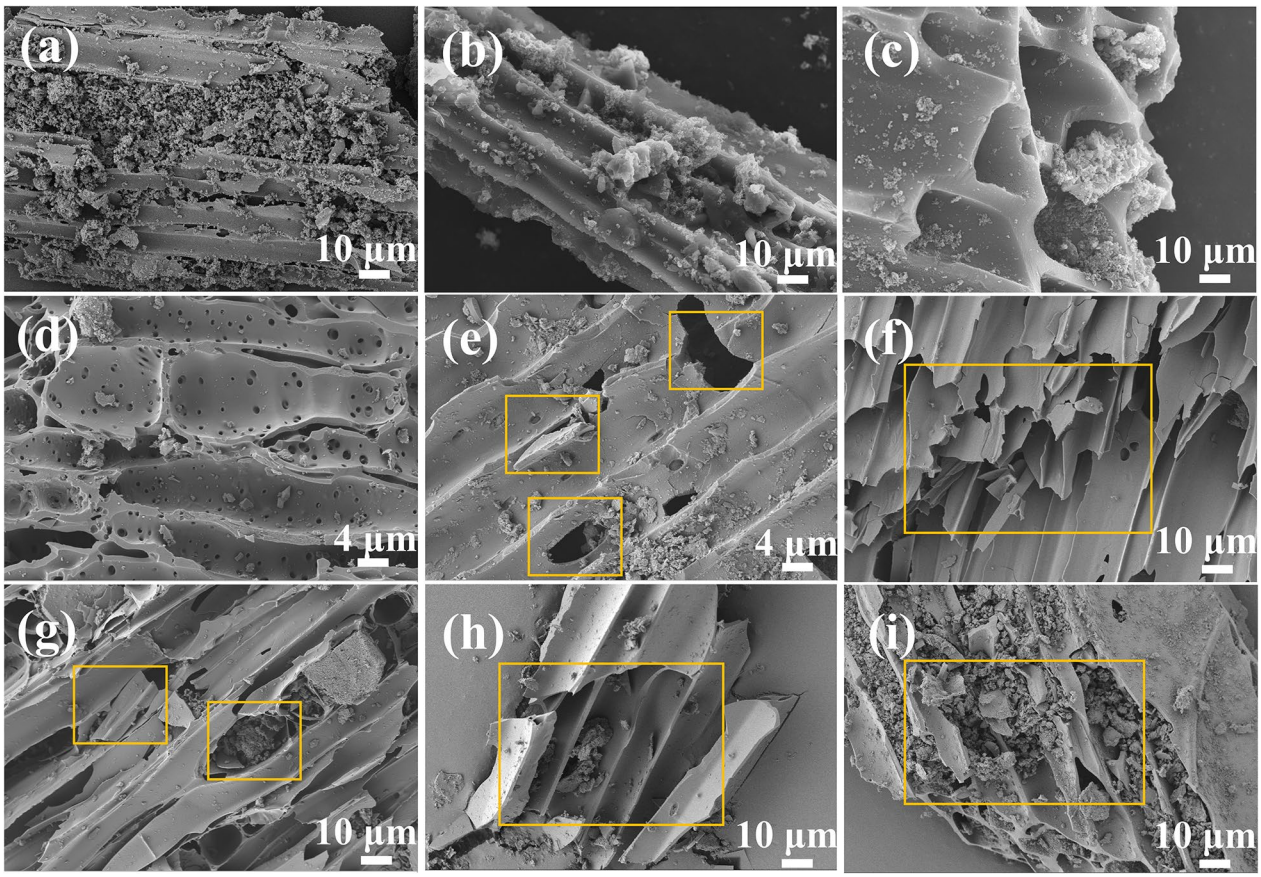

Fig. 1 SEM images of fresh biochar (**a**–**c)** and aged biochar (**d**–**l)** from saline soils. Yellow boxes represent physical change in aged biochar. Yellow boxes of (**e**) local surface rupture, **f** pore structure erosion, **g** pore blockage, **h** structural splitting, and **i** severe pore blockage in the cross sections

pore blockage by soil particles (Fig. 1g), structural splitting that exposed the inner surface and internal structure (Fig. 1h), and severe pore blockage by numerous soil particles in the cross sections (Fig. 1i).

3.2 Variation in elemental and mineral composition of biochar during aging

Figure 2 illustrates changes in the total amounts of C, O, N, and H during biochar aging. The total C content decreased with increasing aging cycles (Fig. 2a), whereas the total O content increased progressively (Fig. 2c). The most pronounced changes were observed in LB, where the C content declined from 54.79% to 29.06%, and the O content increased from 9.39% to 15.94%. The N and H contents (Fig. 2b and e) initially increased but declined in the final cycle. The O/C atomic ratio steadily increased with aging time (Fig. 2f), whereas the H/C ratio initially increased and then decreased (Fig. 2g). Soil salinity significantly influenced C and H contents, whereas aging time had a notable impact on C, H, and O contents. However, there was no significant interaction between salinity and aging time on elemental composition.

Changes in the surface elemental composition of biochar during aging were analyzed semi-quantitatively using XPS (Table 2). After the first aging cycle, the concentrations of Mg, Ca, Fe, Cl, and O decreased in the fresh biochar, whereas those of C and Al increased. Changes in the C content were particularly notable, with surface C levels decreasing significantly from approximately 62% to 36% after three aging cycles, representing a reduction of 20%. No significant changes were observed after the fourth cycle. The surface O and Si contents gradually increased, with O increasing by approximately 3%. In addition, Mg, Na, Fe, and Cl were detected on the surface of aged biochar after three cycles. Soil salinity significantly affected surface levels of Mg, Ca, Na, and Fe, whereas most surface elements exhibited substantial changes with aging time. The interaction between soil salinity and aging time was significant for Mg, Al, Ca, Na, Fe, and Cl concentrations.

Figure S2 shows that the characteristic peaks of quartz (SiO_2) and calcite ($CaCO_3$) were more prominent in aged biochar than in fresh biochar, indicating that quartz and calcite were the primary crystalline phases in aged

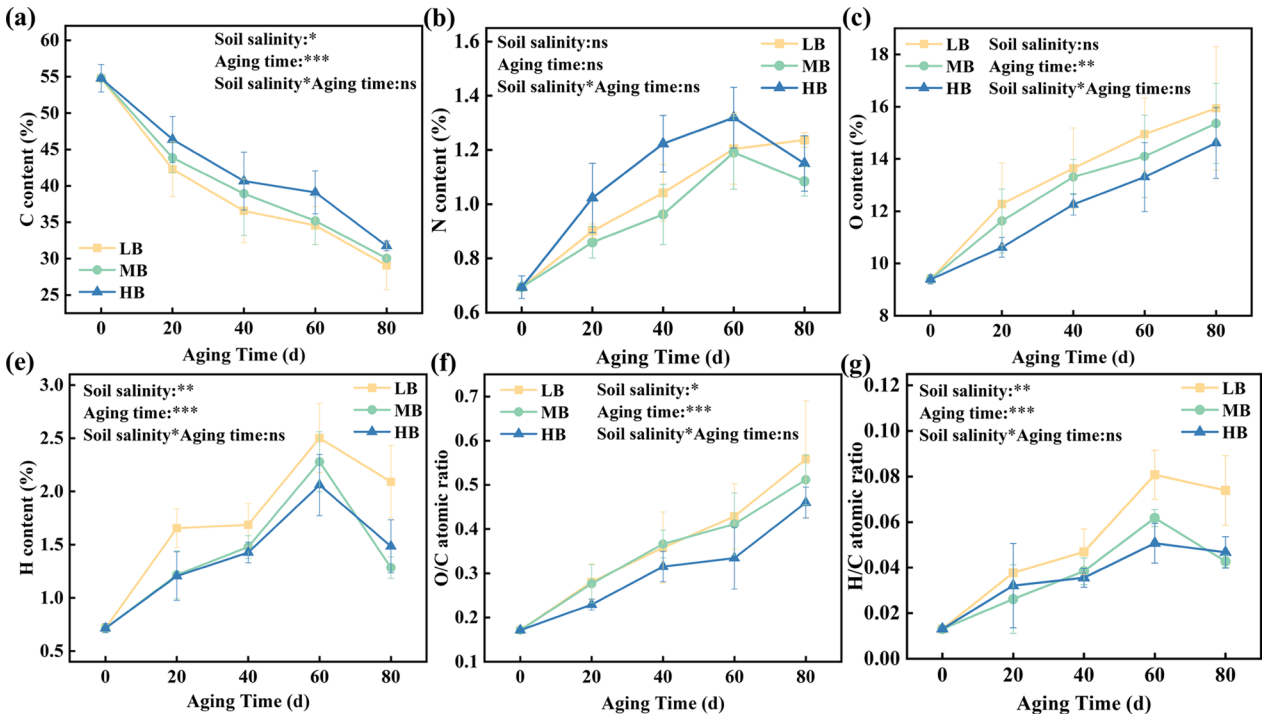

Fig. 2 Total elemental content of biochar aged in saline soils. **a** Total C content, **b** total N content, **c** total O content, **d** total H content, **f** O/C atomic ratio, and **g** H/C atomic ratio. $p < 0.001$***, $p < 0.01$**, $p < 0.05$*

Table 2 Surface element content of biochar aged in saline soils (%)

Sample	O	C	Si	Mg	N	Al	Ca	Na	Fe	Cl
FB	26.07	56.01	3.61	2.83	1.50	——	3.42	0.86	——	2.86
LB1	17.61	61.53	2.54	——	2.69	2.10	1.27	——	——	——
MB1	17.04	62.83	2.02	——	2.60	2.54	0.87	——	——	——
HB1	17.50	63.18	3.10	——	2.69	2.98	2.18	——	——	——
LB2	18.90	48.39	2.68	——	2.25	3.12	1.18	——	——	——
MB2	18.57	53.93	2.27	——	2.70	2.29	1.21	——	——	——
HB2	18.58	54.99	2.36	——	2.76	2.84	1.29	——	——	——
LB3	19.43	36.78	3.58	0.62	2.57	2.21	0.94	0.31	——	——
MB3	20.21	35.73	4.03	0.84	1.97	2.19	1.14	0.40	0.70	——
HB3	19.52	37.17	3.66	0.87	1.92	2.33	1.01	0.56	0.76	——
LB4	19.69	35.87	3.81	0.70	2.73	2.10	0.92	0.21	0.60	0.44
MB4	19.71	35.70	3.69	0.79	3.30	2.18	1.06	0.29	0.51	0.52
HB4	21.21	35.55	3.83	0.87	3.48	2.16	1.06	0.42	0.60	0.54
Soil salinity	ns	ns	ns	**	ns	ns	**	**	*	ns
Aging time	*	***	ns	***	***	ns	**	***	***	***
Soil salinity* Aging time	ns	ns	ns	**	ns	*	***	*	**	ns

"——" indicates not detected. $p < 0.001$***, $p < 0.01$**, $p < 0.05$*

biochar. During the aging process, biochar absorbed substantial amounts of soil minerals including Fe_2O_3, SiO_2, CaO, and Al_2O_3 (Table S3).

We analyzed the correlation matrix of soil salinity with elemental and mineral compositions during biochar aging (Fig. S4). For the elemental composition of the aged biochar, significant correlations with salinity

were observed for total C ($r=0.419$, $p=0.03$), total O ($r=-0.345$, $p=0.018$), O/C ($r=-0.572$, $p=0.006$), H/C ($r=-0.634$, $p=0.004$), surface Mg ($r=0.503$, $p=0.001$), surface Fe ($r=0.439$, $p=0.027$), and surface Cl ($r=0.378$, $p=0.029$). For mineral composition, significant correlations with salinity were identified for K_2O ($r=0.234$, $p=0.01$), ZnO ($r=0.571$, $p=0.006$), SO_3 ($r=0.947$, $p=0.01$), and P_2O_5 ($r=0.612$, $p=0.015$).

3.3 Variation in surface functional groups during biochar aging

Figure 3 illustrates changes in the functional groups during biochar aging in saline soils. The characteristic C–O–C stretching vibration peak (1156 cm^{-1}) associated with cellulose and hemicellulose was observed only in the fresh biochar and disappeared in all aged biochar samples. In contrast, aged biochar exhibited several intensified peaks that became sharper over time, including aliphatic $-CH_2-$ (2861 and 2981 cm^{-1}), carboxyl C=O (1627 cm^{-1}), C–O or Si–O (1025 cm^{-1}), C–H aromatic ring oscillations (780 cm^{-1}), Al–O–Si (524 cm^{-1}), and Si–O–Si vibrations (468 cm^{-1}). Some peaks, such as –OH (3421 cm^{-1}), carbonyl C=O or $-OH_{deformationvibration}$ (1436 cm^{-1}), and C–H aromatic out-of-plane bending (878 cm^{-1}), initially attenuated and later intensified. As salinity increased, several peaks exhibited significant variations across different saline soils, particularly the carbonyl C=O or $-OH_{deformationvibration}$ (1436 cm^{-1}) and C–O or Si–O (1025 cm^{-1}).

The concentrations of functional groups during biochar aging in saline soil were analyzed semi-quantitatively from C1s deconvolution spectra obtained by XPS (Fig. 4), with specific parameters detailed in Table S4. The identified functional groups included aliphatic/aromatic carbon (C–C/C=C) at 284.8 eV, hydroxyl (C–O) at 286 eV, ketone (C=O) at 287 eV, carboxylic acid/ester (O=C–O) at 289 eV, and carbonate (CO_3^{2-}) at 289.4 eV. During aging, the C–C/C=C content decreased from 50% to approximately 30–40%, with significant differences observed among biochars derived from different saline soils, increasing with salinity. Notably, a 10% difference was observed between LB and HB. The oxygen-containing functional groups exhibited varying degrees of increase, with C=O and CO_3^{2-} demonstrating the most notable changes, increasing by 16.13% and 4.76%, respectively. Although the C–O and O–C=O contents initially decreased, they gradually increased over time. Multivariate ANOVA revealed that salinity did not significantly affect most of the functional groups. However, aging time had a significant effect. In addition, salinity and aging time showed significant interactive effects only on CO_3^{2-}. Significant correlations were identified between salinity and C–C content ($r=0.311$, $p=0.022$), as well as C–O content ($r=-0.217$, $p=0.032$) (Fig. S4).

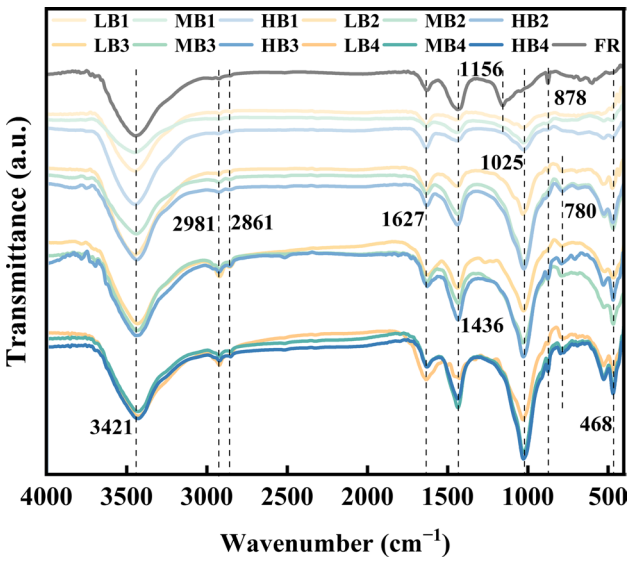

Fig. 3 FTIR spectra of biochar aged in saline soils

3.4 Microbial community colonization of biochar after aging

The microbial responses within the biochar microdomains during aging were analyzed. qPCR analysis detected amplified bands in the aged biochar, whereas no amplification was observed in the fresh biochar (Fig. S5). After four aging cycles, microbial communities in the biochar microhabitat were characterized (Fig. 5). Figure 5a illustrates that LB4 exhibited a significantly higher fungal gene copy number than both MB4 and HB4. The effects of salinity on bacterial and fungal community structures of aged biochar were analyzed using PCoA at the genus level and compared with those of the soil community (Fig. 5c). Microbial communities in biochar were significantly separated from those in soil, as further confirmed by PERMANOVA, highlighting marked differences in microbial community structures between biochar and soil. The Chao1 index for biochar bacteria ($p<0.001$) and fungi ($p<0.05$) differed significantly across soils with varying salinity levels (Fig. 5d). Bacterial and fungal communities in LB4 exhibited higher Chao1 indices than those in MB4 and HB4. However, the Shannon index demonstrated no significant differences among treatments (Fig. 5d). Significant correlations with salinity were observed for fungal gene copies ($r=-0.762$, $p=0.028$), bacterial Chao1 index ($r=-0.700$, $p=0.036$), and fungi Chao1 index ($r=-0.400$, $p=0.048$).

To examine differences in microbial community composition between aged biochar and soil, the dominant bacterial and fungal phyla in the aged biochar (Fig. 5b)

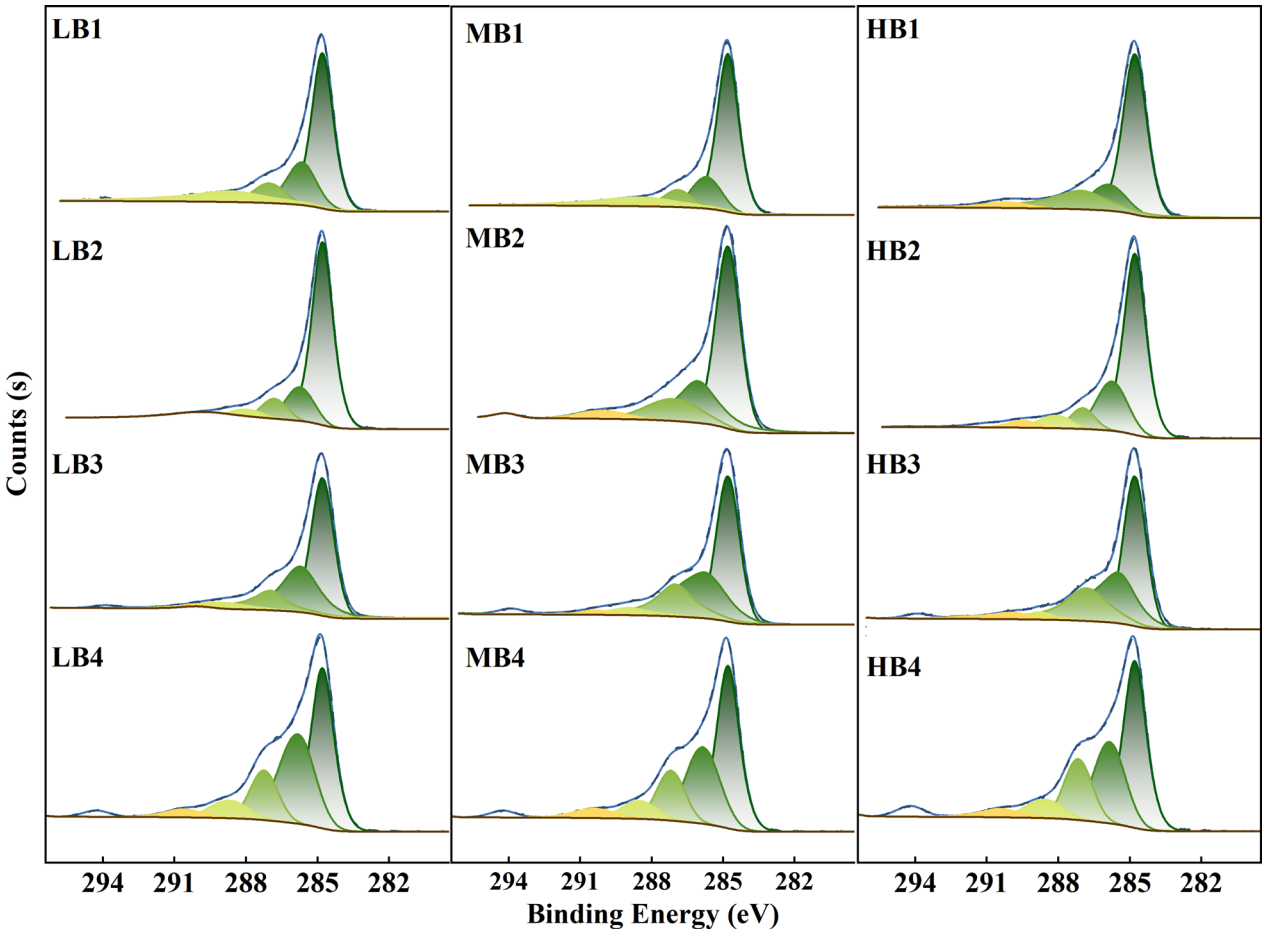

Fig. 4 C1s XPS deconvolution spectra of biochar aged in saline soils

and soil (Fig. S6) were compared. The abundances of Firmicutes and Planctomycetota in biochar were higher than those in soil across all salinity gradients, with specific values provided in Table S3. The relative abundance of Bacteroidetes was higher in LB4 than that in LS4. In contrast, the abundance of Verrucomicrobiota decreased with increasing salinity in the soil community but increased in biochar with rising salinity. Blastocladiomycota was the dominant fungal phylum in the biochar, whereas its relative abundance in the soil was notably low. The relative abundance of Basidiomycota in biochar was much higher than that in the soil, except under high salinity. In contrast, the abundance of Ascomycota in biochar was substantially lower than that in soil under low and moderate salinity but not in high-salinity soils. To further clarify the differences in microbial abundance and composition of aged biochar across salinized soils, a genus-level analysis of microbial communities was conducted (Fig.S7). In the bacterial community, 10 dominant genera, including *Pontibacter*, *Pseudomonas*, and *Ramlibacter*, exhibited significant variations influenced by salinity levels. In the fungal community, only *Preussia* showed significant differences. RDA revealed the impact of biochar characteristics on colonizing microorganisms (Fig. 5f). The results demonstrated significant correlations between the bacterial community and biochar properties, including C–C/C–C content ($p=0.004$) and O/C ratio ($p=0.002$). Figure 5g shows the explanatory power of biochar microbial community indicators on biochar properties. Fungal gene copy number ($p=0.012$) and fungal Chao1 index ($p=0.012$) were significantly positively correlated with biochar properties including C–O, H, and O content, while showing significant negative correlations with C content and C–C content.

Microbial ecological networks were constructed for the bacterial (Fig. 6a) and fungal (Fig. 6b) communities in the aging biochar (Table S4). All six microbial networks conformed to a lognormal distribution model. In the bacterial community, the number of network edges, average degree, clustering coefficient, and network density were lower in LB4 than in MB4 and HB4, indicating lower bacterial network complexity under lower

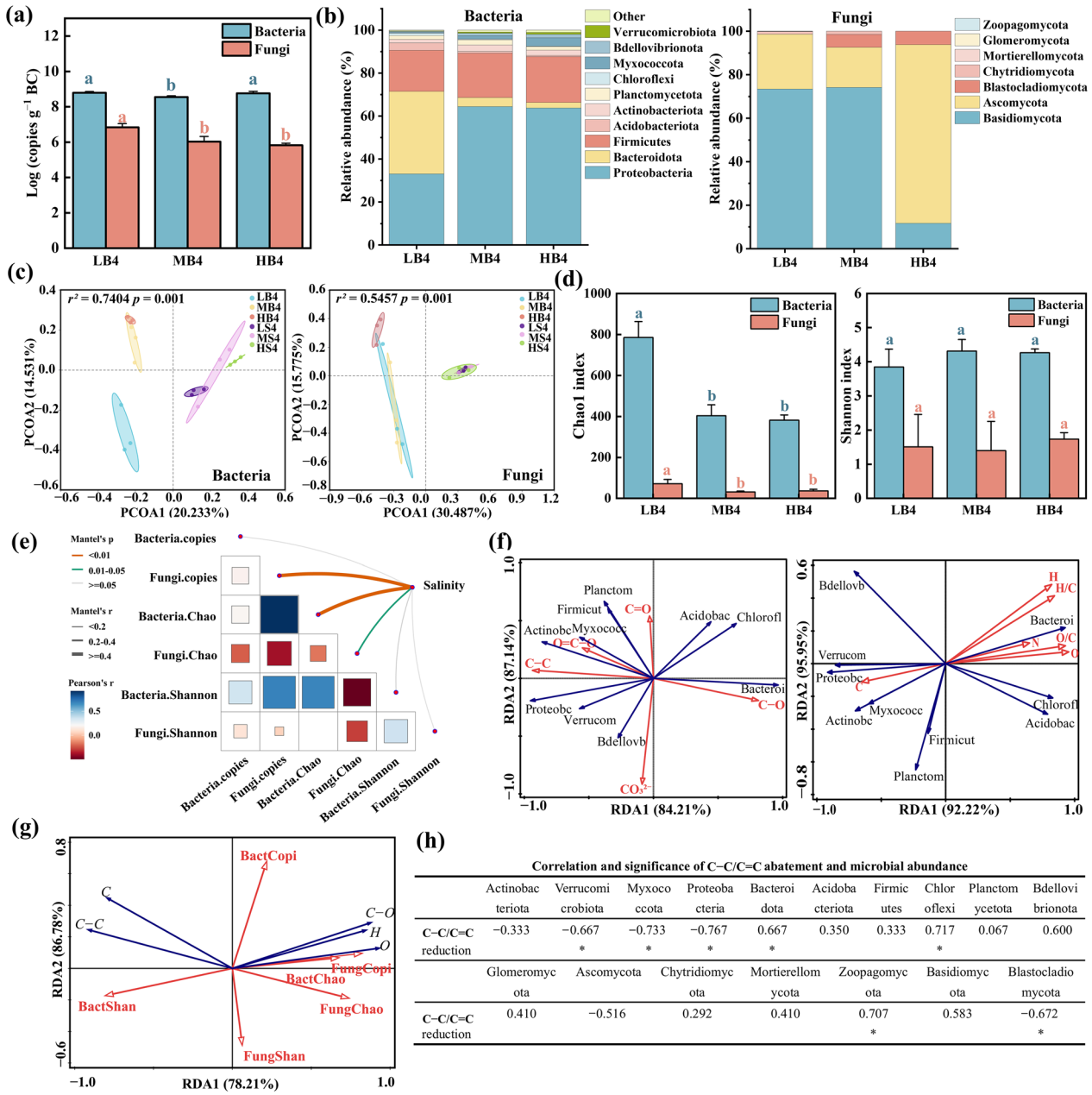

(h)

Correlation and significance of C–C/C=C abatement and microbial abundance

	Actinobacteriota	Verrucomicrobiota	Myxococcota	Proteobacteria	Bacteroidota	Acidobacteriota	Firmicutes	Chloroflexi	Planctomycetota	Bdellovibrionota
C–C/C=C reduction	−0.333	−0.667 *	−0.733 *	−0.767 *	0.667 *	0.350	0.333	0.717 *	0.067	0.600

	Glomeromycota	Ascomycota	Chytridiomycota	Mortierellomycota	Zoopagomycota	Basidiomycota	Blastocladiomycota
C–C/C=C reduction	0.410	−0.516	0.292	0.410	0.707 *	0.583	−0.672 *

Fig. 5 **a** Gene copy number. **b** Microbial community composition at the phylum level. **c** Principal coordinate analysis. **d** Alpha diversity indices of bacteria and fungi. **e** Correlation between microbial community indicators and soil salinity. **f** Redundancy analysis (RDA) of biochar properties (explanatory variables) and species (response variables). **g** Redundancy analysis (RDA) of biochar properties (explanatory variables) and microbial indicators (response variables). **h** Correlation between C–C/C = C abatement and microbial abundance in aged biochar from different saline soils

salinization conditions. In contrast, in the fungal community, the number of network edges, average degree, and network density in the aging biochar decreased with increasing salinity while average path length increased, reflecting a decline in fungal network complexity under higher salinity. Positive correlations among bacterial species decreased, whereas negative correlations increased with increasing salinity, suggesting that intensified salinization enhanced antagonistic or competitive relationships within the bacterial community, which may contribute to greater community stability. However, this represents only indirect statistical evidence, and true ecological antagonistic interactions require further experimental validation. Resistance of microbial networks to

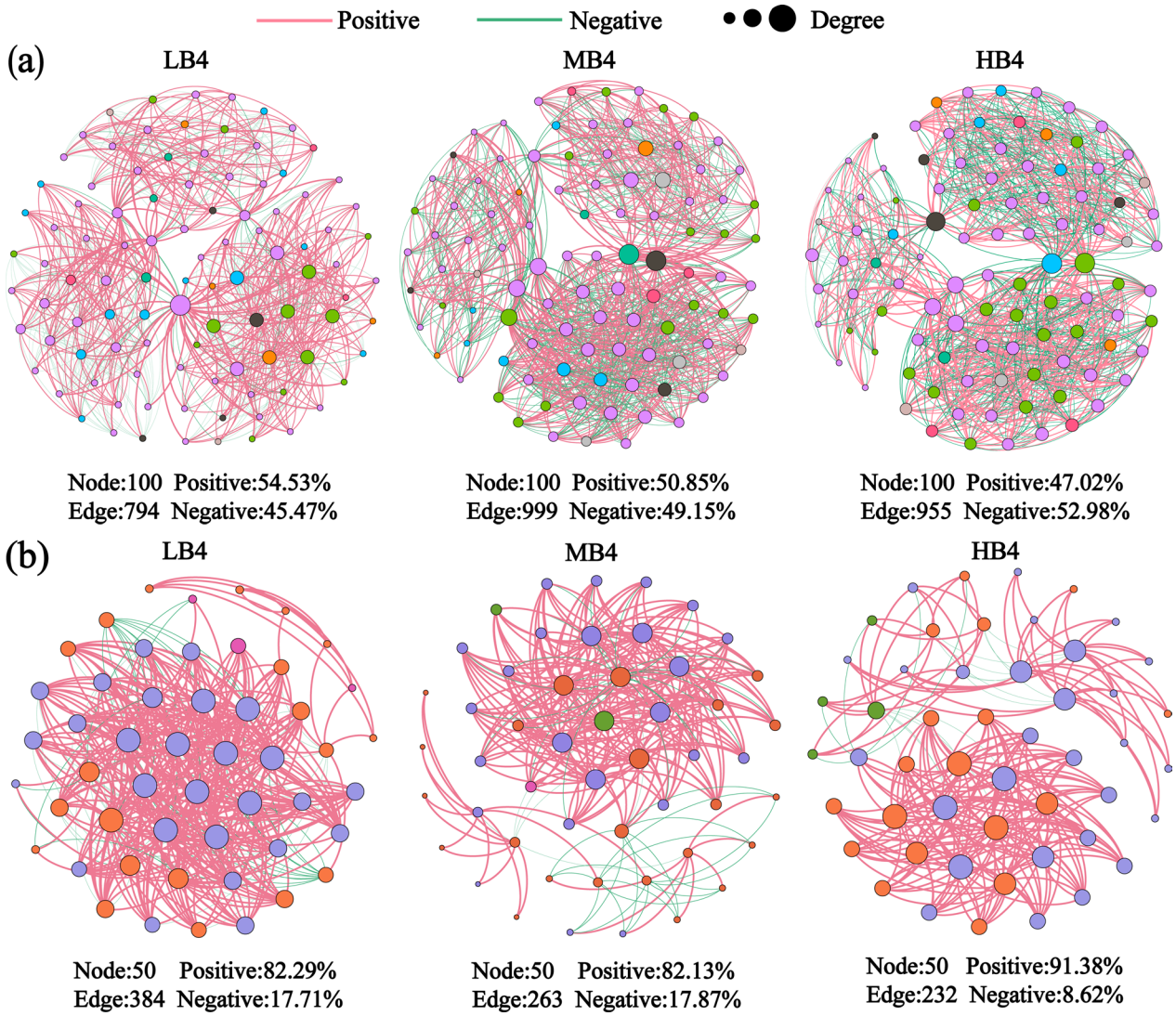

Fig. 6 Co-occurrence network of **a** bacterial and **b** fungal communities in aged biochar

disturbances was also tested by robustness analysis (Fig. S9). We found that the natural connectivity of bacterial networks decreased to a greater degree in LB4 by removing the same proportion of nodes or edges, indicating weakened resistance under low salinity (Fig.S9). Conversely, fungal networks in the HB4 treatment demonstrated the weakest robustness, suggesting that high-salinity conditions have a pronounced negative impact on fungal network stability.

4 Discussion

4.1 Mechanisms of biochar aging at different stages in saline soils

Shortly after fresh biochar was applied to saline soils, inorganic salt dissolution and loss of unstable carbon, including dissolved organic matter (DOM) and dissolved black carbon (DBC), were observed (Dong et al. 2017; Spokas et al. 2014). This was supported by changes in surface elements (Table 2), the disappearance of cellulose C–O–C functional groups (Fig. 3), and a reduction in the C–O peak area (Table S2) in fresh biochar (Yi et al. 2020). The total carbon content of biochar decreased by approximately 20%, primarily because of the dissolution of unstable C and mineralization of organic carbon (Dai et al. 2021; Quan et al. 2020). Previous research has indicated that microbial abundance is positively correlated with aliphatic C but negatively correlated with aromatic C in biochar (Zhang et al. 2018). The substantially unstable C provided by biochar during the initial phase can serve as a carbon source for microorganisms, whereas

recalcitrant aromatic carbon in later phases is decomposed into humus and other compounds (Yi et al. 2020; Bandara et al. 2021; Zimmerman 2010). In this study, the initial C loss predominantly occurred on the biochar surface, resulting in a significant reduction in the surface C content during the first three cycles (Li et al. 2019). Subsequent C loss likely resulted from the depletion of unstable C on the exposed inner surfaces of the biochar and microbial degradation of recalcitrant C.

The total O content of the biochar increased by approximately 5%, which was attributed to the oxidation of aromatic groups and the formation of oxygen-containing functional groups such as hydroxyl, carboxyl, and carbonyl groups (Mia et al. 2017b; Chen et al. 2023). Soil microbial decomposition breaks unstable aliphatic chains, which release free aromatic fractions and form functional groups at the breakpoints (Zimmerman 2010; Kuzyakov et al. 2014; Hilscher et al. 2009). This was supported by FTIR and XPS analyses, which showed a decrease in the C–C/C=C ratio and an increase in the C–O, C=O, and O=C–O bonds. Additionally, biochar can adsorb CO_2 from the environment, thereby contributing to the formation of new CO_3^{2-} (Xu et al. 2016). During aging, the increase in H and N contents on the surface of aged biochar could be attributed to the adsorption of organic matter and mineral nutrients (Li et al. 2019). The adsorption of H and degradation of aromatic carbon also led to an increased H/C ratio, indicating reduced aromaticity (Yi et al. 2020; Tan et al. 2020). The rapid decline observed in the final stage may be due to extensive microbial colonization and the rapid utilization of aliphatic carbon.

4.2 Effect of different salinization on microorganisms colonizing biochar

The porous structure of biochar acts as a "shelter" for soil microorganisms, supporting their survival and reproduction (Gul et al. 2015). Microbial colonization within biochar is facilitated by the abundance of nutrients, including unstable C and minerals, which are carried and adsorbed by the biochar (Dai et al. 2021). This colonization is further enhanced when powdered biochar is used instead of coarse lumps (Quilliam et al. 2013). Although fresh biochar contains high concentrations of mineral salts and PAHs that are unfavorable for microbial survival, microbial colonization readily occurs on aged biochar, consistent with previous findings (Quilliam et al. 2013; Luo et al. 2013).

This study demonstrated that soil salinization exerted distinct effects on the activity, diversity, and stability of bacterial and fungal communities in aged biochar. Fungal community biomass in aged biochar declined with increasing salinity, indicating that soil salinity significantly inhibited fungal activity (Zhu et al. 2025). In contrast, bacterial community biomass showed no significant correlation with salinity, suggesting that bacterial activity was less sensitive to salinity stress, potentially because SOM can mitigate the effects of salinity on microorganisms (Rath et al. 2019). The pattern of declining microbial species richness coupled with unchanged species diversity indicated that rare, low-abundance taxa were lost under higher salinity, whereas the relative abundances of dominant taxa remained stable. This suggests that salinity eliminated sensitive rare taxa but retained the salt-tolerant core community (Yang et al. 2025). From a functional perspective, the loss of rare taxa can potentially weaken the community's functional redundancy, thereby reducing its resilience to subsequent environmental disturbances and its functional diversity (Shade et al. 2014). Integrated with the RDA results (Fig. 5f, g), microbial richness was correlated with the C and O elements of biochar, suggesting a connection between changes in microbial diversity and functional shift in carbon degradation.

Studies of microbial co-occurrence networks have shown that the complexity and stability of bacterial and fungal communities within biochar are regulated by soil salinity and exhibit contrasting trends. With increasing salinity, the complexity and stability of fungal communities are significantly reduced, whereas those of bacterial communities are enhanced. This pattern may not be solely attributable to salinity-driven selection, as previous studies have shown that fungal communities are often more stable than bacterial communities under salt stress (Rath et al. 2019). We propose three underlying mechanisms. Firstly, the constraint of the labile carbon pool. Biochar aged in high-salinity soils retains greater amounts of labile C, which strengthens species interactions and sustains bacterial network complexity and stability. In contrast, increased competition for resources in low-salinity environments leads to a simplified network structure and a vulnerable system (Sun et al. 2025). Secondly, the fundamental differences in bacterial and fungal responses to salt stress in specific microhabitats. The micropores of biochar are unfavorable for the establishment of fungal hyphal networks (Ruamps et al. 2011). High salinity can damage fungal hyphae and eliminate keystone species, ultimately causing network collapse. Conversely, bacterial communities are filtered by high salinity to form a tightly interconnected network composed of salt-tolerant specialists (Wang et al. 2026). Thirdly, the impediment of microbial community succession. A successional shift from bacterial to fungal dominance is expected during biochar aging. Initially, labile carbon sources (e.g., DOC and aliphatic C) promote rapid bacterial colonization. As these substrates deplete, fungi,

capable of degrading recalcitrant C (e.g., aromatic compounds), are theorized to increase and become dominant (Dai et al. 2021; Parasar et al. 2025). We hypothesize that high salinity stress impedes this natural successional progression. Future studies monitoring microbial dynamics over time are crucial to validate the occurrence of such succession.

There is evidence that the characteristics of biochar influence the colonization of specific microbial species, leading to variations in their abundance compared with soil microbes. PCoA revealed significant differences in the microbial community composition between the biochar microhabitat and the soil microbial community, likely because of the distinct characteristics of biochar and the unique environment it provides for microorganisms. Biochar associated with microorganisms can serve as a carbon source (Dai et al. 2021; Watzinger et al. 2014; Kuzyakov et al. 2009). Firmicutes stably colonize biochar, likely due to their strong ability to utilize both labile and recalcitrant forms of organic carbon, enabling them to rapidly establish and persist on biochar (Parasar et al. 2025; Liao et al. 2019; Ling et al. 2021). Planctomycetota also showed potential for the degradation of complex carbohydrates in biochar. Studies have shown that they possess a variety of polysaccharide-degrading enzymes, and their abundance is positively correlated with carbon emissions in saline-alkali soils (Klimek et al. 2024; Zhang et al. 2024a, b). Bacteroidota and Blastocladiomycota are strongly linked to cumulative carbon mineralization in biochar-amended soils owing to their lignin- and cellulose-degrading abilities (Zhao et al. 2021; Fan et al. 2024; López-Mondéjar et al. 2016), demonstrating high colonization of biochar. Verrucomicrobiota can degrade lignin, xylan, polysaccharides, and hemicellulose, potentially driving carbon turnover (Rakitin et al. 2024; Brewer et al. 2016; Tan et al. 2025). The high aliphatic and aromatic carbon contents in biochar from highly saline soils may also facilitate the colonization of Verrucomicrobiota. This suggests that although Verrucomicrobiota may experience salt stress in soil, the abundant carbon sources in biochar help mitigate the negative effects of salinity. Ascomycota and Basidiomycota include saprotrophic fungi capable of degrading aromatic compounds, contributing to the decomposition and mineralization of biochar (Parasar et al. 2025; Yin et al. 2023). However, the observed shift in their relative abundances between soil and biochar suggests that Basidiomycota may be the dominant fungal group responsible for breaking down recalcitrant aromatic C in biochar, consistent with previous findings (Noyce et al. 2016; Bai et al. 2024). Under high salinity conditions, the high abundance of Ascomycota in biochar indicates their strong salt tolerance, whereas the colonization of Basidiomycota on biochar appears to be inhibited by salt stress (Yang et al. 2020). Therefore, under high salinity conditions, Ascomycota play a more important role in C catabolism.

4.3 Effects and mechanisms of different salinization on biochar aging

This study demonstrated that soil salinity significantly influenced various biochar properties (Fig. S4), including elemental composition and surface functional groups. Saline soils affect biochar both directly through salinity and indirectly through other soil characteristics. The total C and surface aliphatic/aromatic C contents of biochar increased with increasing salinity, whereas the total O content, oxidability, and surface ether bonds/hydroxyl groups decreased. This suggests that higher salinity may slow biochar aging, potentially due to reduced microbial community activity, which slows carbon degradation, specifically the decomposition and mineralization of unstable aliphatic C, as well as the cleavage and degradation of recalcitrant aromatic groups. The limited number of oxidizable aromatic cleavage sites further slows the oxidation of biochar (Ge et al. 2024; Rath et al. 2019; Zhang et al. 2024a). Consequently, in highly saline soils, the biological aging of biochar is diminished, resulting in higher C content and lower oxidability. Meanwhile, the slow degradation rate of aromatic carbon in biochar leads to an increase in the aromaticity of aged biochar with rising salinity. Previous studies that reported a significant positive correlation between soil microbial biomass and the H/C and O/C atomic ratios of biochar lend support to our findings (Zhang et al. 2018). The RDA analysis (Fig. 5g) further corroborated this conclusion, suggesting that fungal community activity and richness are likely the key factors driving biochar carbon degradation and the enrichment of oxygen-containing functional groups. Fungal communities appear to play a dominant role in the biochar aging process, which is consistent with previous findings (Zhang et al. 2018). As discussed in Sect. 4.2, bacteria such as Firmicutes, Planctomycetota, Bacteroidota, Blastocladiomycota, and Verrucomicrobiota along with fungi such as Basidiomycota may play important roles in driving biochar carbon degradation. Additionally, correlation analysis (Fig. 5f) suggested that bacterial phyla such as Bacteroidetes, Chloroflexi, Verrucomicrobiota, Myxococcota, and Proteobacteria, along with fungal phyla such as Zoopagomycota and Blastocladiomycota, drove the decomposition of aliphatic and aromatic carbon in biochar. These results indicate that microorganisms involved in biochar aging can decompose biochar. Although many studies have focused on organic content and degradation products over specific time scales, few have investigated the underlying mechanisms of microbially driven processes.

As minerals were dissolved and/or ions were exchanged onto the external surfaces of biochar, they adhered tightly to its surface through physical adsorption (Ren et al. 2018). XRD/XRF analysis further supported the mineral deposition hypothesis (Fig. S2 and Table S3). After aging, the surface of biochar became enriched with quartz and calcite crystalline phases as well as substantial amounts of soil minerals. Such mineral enrichment likely contributed to the formation of a physical barrier that impeded further oxidative transformation, thereby retarding the aging process. We observed positive correlations between surface elemental and mineral concentrations (e.g., Mg, Na, Fe, Cl, and ZnO) and the degree of salinization (Figs. S4b and S4d), indicating that in highly saline soils, salts preferentially accumulate on aged biochar surfaces to form a continuous protective layer. Li et al. demonstrated that calcium salts or minerals deposited within biochar pores can reduce carbon loss by more than 10%, thereby enhancing carbon retention and overall stability of the biochar matrix (Li et al. 2014). Beyond acting as physical barriers, soil salts and minerals can interact with biochar surfaces through chemical bonding or infiltration of internal pores, leading to the formation of stable organometallic complexes (Giannetta et al. 2024). FTIR analysis revealed the emergence of new Al–O–Si characteristic peaks that gradually intensified over time in aged biochar, indicating continuous interactions between biochar and soil minerals during aging (Jing et al. 2022). Negatively charged biochar can bind positively charged species such as iron hydroxides, forming Fe–O–C linkages that further enhance oxidation resistance (Giannetta et al. 2024). Aromatic structures in biochar can associate with mineral components to form stable organo–mineral complexes, thereby improving carbon stability (Yang et al. 2021). Yang et al. found that Cl diffused into the biochar interior after 1 year, suggesting deep integration of mineral species (Yang et al. 2016). In this study, elements such as Fe, Mg, and Cl were enriched with increasing salinity, potentially promoting the formation of organometallic complexes. These two mechanisms, physical surface shielding and chemical complexation, act synergistically to enhance the oxidation resistance of the biochar and reduce its surface reactivity.

By integrating previous studies on biochar aging in non-saline soils, both similarities and differences in the aging mechanisms of biochar in saline and non-saline soils can be identified. Similarities include the leaching and microbial decomposition of labile carbon during the early stages, microbial degradation of recalcitrant carbon during the later stages, and protection by mineral barriers (Zhang et al. 2018; Yang et al. 2021). The differences lie in the accumulation of salts in saline soils, where salt stress reduces the activity of indigenous soil microorganisms compared with non-saline soils, thereby slowing the biochar aging process. In addition, the coverage and adsorption of salts on the biochar surface effectively protect it from oxidation. Finally, salinization can alter the abundance of specific microbial taxa, such as Firmicutes and Ascomycota, which may in turn affect the rates of certain biochar aging pathways (Yang et al. 2020).

4.4 Implications for biochar application in saline soils and future prospects

Biochar undergoing long-term aging in saline soils not only exhibits distinct alterations in properties and microbial colonization but is also strongly influenced by varying levels of salinization. Long-term biochar aging can improve soil characteristics, such as fertility, nutrient retention capacity, and crop productivity (Jin et al. 2024; Wang et al. 2025). Oxygenated functional groups on biochar surfaces enhance the retention of cations and other nutrients through adsorption and ligand exchange (Mao et al. 2012). In addition, biochar aging promotes complexation with soil minerals and stabilization of soil organic matter (Yang et al. 2016; Fang et al. 2015). Furthermore, aged biochar provides an ideal habitat for microbial communities and increases microbial diversity, both of which are crucial for the functional improvement of saline soils (Mao et al. 2022; Wang et al. 2024). However, recent research has shown that biochar produces environmentally persistent free radicals that are toxic to soil microorganisms (Yang et al. 2023). In highly salinized soils, biochar exhibits greater stability, which helps reduce soil carbon emissions and supports long-term carbon sequestration (Luo et al. 2023; Major et al. 2010). Therefore, in highly salinized soils, biochar application is a promising strategy for improving soil properties from a long-term and sustainable perspective. It promotes soil aggregate formation and carbon sequestration, thus showing great potential for enhancing soil fertility (Jia et al. 2024; Trozzo et al. 2025).

Although some novel phenomena were observed, this study has several methodological limitations. First, the aging process was simulated solely through wet–dry cycles, without considering other natural factors such as temperature, sunlight, and freeze–thaw cycles. This might lead to an underestimation of the actual aging rate in field environments. Therefore, long-term natural aging experiments in actual field settings are required. Second, the absence of quantitative indicators related to carbon mineralization, aliphatic/aromatic C contents, and microbial activity prevented the provision of direct evidence for the pathways through which microorganisms influence the rate of biochar aging. Third, dynamic changes in microbial communities within the biochar were not continuously tracked across

multiple time points, making it difficult to explore shifts in microbially driven aging mechanisms at different stages. Although the design aimed to highlight the influence of salinization gradients on biochar-associated microbes, it overlooked the temporal dynamics of salinity effects on soil microorganisms. Future studies should provide direct evidence to clarify the detailed pathways of microbially driven biochar aging in saline soils, particularly under natural environmental conditions and dynamic changes.

5 Conclusions

This study demonstrates that soil salinity significantly decelerates the aging process of biochar, as evidenced by reduced oxidation, higher retention of aromatic carbon, and lower microbial colonization, particularly of fungi, in high-salinity environments. The aging retardation is attributed to both microbial inhibition and the physical barrier formed by salt-mineral coatings on biochar surfaces. These findings highlight the role of salinity in modulating biochar–microbe interactions and its long-term stability in saline soils. We suggest that aged biochar has the potential to improve highly saline soil properties. However, this study has certain limitations. The aging simulation relied solely on wet–dry cycles, omitting other environmental factors such as temperature and sunlight exposure, which may underestimate field aging rates. Moreover, the lack of direct measurements of carbon mineralization and microbial activity limits mechanistic insight into aging pathways. Future research should incorporate multi-factor aging experiments, track microbial succession dynamically, and quantify carbon transformation pathways to better predict the long-term behavior of biochar in saline agroecosystems.

Supplementary Information

The online version contains supplementary material available at https://doi.org/10.1007/s42773-026-00589-w.

Supplementary Material 1.

Author contributions

Ruoyu Wang: Methodology, Data curation, Formal analysis, Investigation, Visualization, Writing—original draft. Hongqiang Li: Formal analysis, Methodology. Naqi Cui: Formal analysis, Methodology, Visualization. Tang Chong: Formal analysis, Methodology. Wenping Xie: Supervision, Project administration. Xiangping Wang: Supervision, Project administration. Rongjiang Yao: Conceptualization, Supervision, Funding acquisition, Writing—review and editing.

Funding

This work was supported by the National Natural Science Foundation of China (32271720) and National Key Research and Development Program of China (2021YFD1900602 and 2021YFC3201201).

Data availability

The raw sequencing data and key physicochemical datasets have been uploaded to Mendeley Data under https://doi.org/10.17632/f2yn5jjk43.1.

Declarations

Competing interests

The authors declare that they have no conflict of interest.

Author details

[1]State Key Laboratory of Soil and Sustainable Agriculture, Institute of Soil Science, Chinese Academy of Sciences, Nanjing 210008, Jiangsu, China. [2]State Key Laboratory of Urban and Regional Ecology, Research Center for Eco-Environmental Sciences, Chinese Academy of Sciences, Beijing 100085, China.

Received: 25 March 2025 Revised: 16 January 2026 Accepted: 2 February 2026
Published online: 09 March 2026

References

Bai X, Zhang E, Wu J, Ma D, Zhang C, Zhang B, Liu Y, Zhang Z, Tian F, Zhao H, Wang B (2024) Soil fungal community is more sensitive than bacterial community to modified materials application in saline–alkali land of Hetao Plain. Front Microbiol 15:1255536

Bandara T, Franks A, Xu J, Chathurika JBAJ, Tang C (2021) Biochar aging alters the bioavailability of cadmium and microbial activity in acid contaminated soils. J Hazard Mater 420:126666

Brewer TE, Handley KM, Carini P, Gilbert JA, Fierer N (2016) Genome reduction in an abundant and ubiquitous soil bacterium '*Candidatus* Udaeobacter copiosus'. Nat Microbiol 2:16198

Chen X, Gao X, Yu P, Spanu L, Hinojosa J, Zhang S, Long M, Alvarez PJJ, Masiello CA (2023) Rapid simulation of decade-scale charcoal aging in soil: changes in physicochemical properties and their environmental implications. Environ Sci Technol 57:128–138

Cruz-Paredes C, Tájmel D, Rousk J (2021) Can moisture affect temperature dependences of microbial growth and respiration? Soil Biol Biochem 156:108223

Dai Z, Xiong X, Zhu H, Xu H, Leng P, Li J, Tang C, Xu J (2021) Association of biochar properties with changes in soil bacterial, fungal and fauna communities and nutrient cycling processes. Biochar 3:239–254

Dong X, Li G, Lin Q, Zhao X (2017) Quantity and quality changes of biochar aged for 5years in soil under field conditions. CATENA 159:136–143

Esfandbod M, Phillips IR, Miller B, Rashti MR, Lan ZM, Srivastava P, Singh B, Chen CR (2017) Aged acidic biochar increases nitrogen retention and decreases ammonia volatilization in alkaline bauxite residue sand. Ecol Eng 98:157–165

Fan T, Zhang Y, Hu K, Xu S, Zhang A, Xue S, Han J, Wang X (2024) Changes in soil organic carbon and microbial community in saline soil following different forms of straw incorporation. Eur J Soil Sci 75:e13457

Fang Y, Singh B, Singh BP (2015) Effect of temperature on biochar priming effects and its stability in soils. Soil Biol Biochem 80:136–145

Ge M, Wang B, Chen B, Xie H, Sun H, Sun K, Feng Y (2024) Hydrochar and its dissolved organic matter aged in a 30-month rice-wheat rotation system: do primary aging factors alter at different stages? Environ Sci Technol 58:3019–3030

Giannetta B, Plaza C, Galluzzi G, Benavente-Ferraces I, García-Gil JC, Panettieri M, Gascó G, Zaccone C (2024) Distribution of soil organic carbon between particulate and mineral-associated fractions as affected by biochar and its co-application with other amendments. Agric Ecosyst Environ 360:108777

Gul S, Whalen JK, Thomas BW, Sachdeva V, Deng H (2015) Physico-chemical properties and microbial responses in biochar-amended soils: mechanisms and future directions. Agric Ecosyst Environ 206:46–59

Hilscher A, Heister K, Siewert C, Knicker H (2009) Mineralisation and structural changes during the initial phase of microbial degradation of pyrogenic plant residues in soil. Org Geochem 40:332–342

Jia A, Song X, Li S, Liu Z, Liu X, Han Z, Gao H, Gao Q, Zha Y, Liu Y, Wu X, Wang G (2024) Biochar enhances soil hydrological function by improving the pore structure of saline soil. Agric Water Manage 306:109170
Jin F, Piao J, Miao S, Che W, Li X, Li X, Shiraiwa T, Tanaka T, Taniyoshi K, Hua S, Lan Y (2024) Long-term effects of biochar one-off application on soil physicochemical properties, salt concentration, nutrient availability, enzyme activity, and rice yield of highly saline-alkali paddy soils: based on a 6-year field experiment. Biochar 6:40
Jing F, Sun Y, Liu Y, Wan Z, Chen J, Tsang DCW (2022) Interactions between biochar and clay minerals in changing biochar carbon stability. Sci Total Environ 809:151124
Klimek D, Herold M, Calusinska M (2024) Comparative genomic analysis of Planctomycetota potential for polysaccharide degradation identifies biotechnologically relevant microbes. BMC Genomics 25:523
Kuzyakov Y, Subbotina I, Chen H, Bogomolova I, Xu X (2009) Black carbon decomposition and incorporation into soil microbial biomass estimated by ^{14}C labeling. Soil Biol Biochem 41:210–219
Kuzyakov Y, Bogomolova I, Glaser B (2014) Biochar stability in soil: decomposition during eight years and transformation as assessed by compound-specific ^{14}C analysis. Soil Biol Biochem 70:229–236
Li F, Cao X, Zhao L, Wang J, Ding Z (2014) Effects of mineral additives on biochar formation: carbon retention, stability, and properties. Environ Sci Technol 48:11211–11217
Li H, Ye X, Geng Z, Zhou H, Guo X, Zhang Y, Zhao H, Wang G (2016) The influence of biochar type on long-term stabilization for Cd and Cu in contaminated paddy soils. J Hazard Mater 304:40–48
Li H, Lu X, Xu Y, Liu H (2019) How close is artificial biochar aging to natural biochar aging in fields? A meta-analysis. Geoderma 352:96–103
Li X, Wang T, Chang SX, Jiang X, Song Y (2020) Biochar increases soil microbial biomass but has variable effects on microbial diversity: a meta-analysis. Sci Total Environ 749:141593
Li S, Zhao L, Wang C, Huang H, Zhuang M (2023) Synergistic improvement of carbon sequestration and crop yield by organic material addition in saline soil: a global meta-analysis. Sci Total Environ 891:164530
Liao H, Li Y, Yao H (2019) Biochar amendment stimulates utilization of plant-derived carbon by soil bacteria in an intercropping system. Front Microbiol 10:1361
Ling L, Fu Y, Jeewani PH, Tang C, Pan S, Reid BJ, Gunina A, Li Y, Li Y, Cai Y, Kuzyakov Y, Li Y, Su W-q, Singh BP, Luo Y, Xu J (2021) Organic matter chemistry and bacterial community structure regulate decomposition processes in post-fire forest soils. Soil Biol Biochem 160:108311
Liu Y, Chen J (2022) Effect of ageing on biochar properties and pollutant management. Chemosphere 292:133427
Long X-X, Yu Z-N, Liu S-W, Gao T, Qiu R-L (2024) A systematic review of biochar aging and the potential eco-environmental risk in heavy metal contaminated soil. J Hazard Mater 472:134345
López-Mondéjar R, Zühlke D, Becher D, Riedel K, Baldrian P (2016) Cellulose and hemicellulose decomposition by forest soil bacteria proceeds by the action of structurally variable enzymatic systems. Sci Rep 6:25279
Luo Y, Durenkamp M, De Nobili M, Lin Q, Devonshire BJ, Brookes PC (2013) Microbial biomass growth, following incorporation of biochars produced at 350 °C or 700 °C, in a silty-clay loam soil of high and low pH. Soil Biol Biochem 57:513–523
Luo L, Wang J, Lv J, Liu Z, Sun T, Yang Y, Zhu Y-G (2023) Carbon sequestration strategies in soil using biochar: advances, challenges, and opportunities. Environ Sci Technol 57:11357–11372
Major J, Lehmann J, Rondon M, Goodale C (2010) Fate of soil-applied black carbon: downward migration, leaching and soil respiration. Glob Change Biol 16:1366–1379
Manasa MRK, Katukuri NR, Darveekaran Nair SS, Haojie Y, Yang Z, Guo Rb (2020) Role of biochar and organic substrates in enhancing the functional characteristics and microbial community in a saline soil. J Environ Manage 269:110737
Mao JD, Johnson RL, Lehmann J, Olk DC, Neves EG, Thompson ML, Schmidt-Rohr K (2012) Abundant and stable char residues in soils: implications for soil fertility and carbon sequestration. Environ Sci Technol 46:9571–9576
Mao X, Yang Y, Guan P, Geng L, Ma L, Di H, Liu W, Li B (2022) Remediation of organic amendments on soil salinization: focusing on the relationship between soil salts and microbial communities. Ecotoxicol Environ Saf 239:113616
Meiirkhanuly Z, Koziel JA, Bialowiec A, Banik C, Brown RC (2020) The Proof-of-the concept of biochar floating cover influence on swine manure pH: implications for mitigation of gaseous emissions from area sources. Front Chem 8:656
Meng Z, Huang S, Xu T, Deng Y, Lin Z, Wang X (2020) Transport and transformation of Cd between biochar and soil under combined dry-wet and freeze-thaw aging. Environ Pollut 263:114449
Meng Z, Huang S, Lin Z, Mu W, Ge H, Huang D (2022) Cadmium long-term immobilization by biochar and potential risks in soils with different pH under combined aging. Sci Total Environ 825:154018
Mia S, Singh B, Dijkstra FA (2017a) Aged biochar affects gross nitrogen mineralization and recovery: a ^{15}N study in two contrasting soils. GCB Bioenergy 9:1196–1206
Mia S, Dijkstra FA, Singh B (2017b) Chapter One - Long-Term Aging of Biochar: A Molecular Understanding With Agricultural and Environmental Implications. In: Sparks DL (ed) Advances in Agronomy. Academic Press, Cambridge
Noyce GL, Winsborough C, Fulthorpe R, Basiliko N (2016) The microbiomes and metagenomes of forest biochars. Sci Rep 6:26425
Parasar BJ, Agarwala N (2025) Unravelling the role of biochar-microbe-soil tripartite interaction in regulating soil carbon and nitrogen budget: a panacea to soil sustainability. Biochar 7:37
Piao J, Che W, Li X, Li X, Zhang C, Wang Q, Jin F, Hua S (2023) Application of peanut shell biochar increases rice yield in saline-alkali paddy fields by regulating leaf ion concentrations and photosynthesis rate. Plant Soil 483:589–606
Quan G, Fan Q, Zimmerman AR, Sun J, Cui L, Wang H, Gao B, Yan J (2020) Effects of laboratory biotic aging on the characteristics of biochar and its water-soluble organic products. J Hazard Mater 382:121071
Quilliam RS, Glanville HC, Wade SC, Jones DL (2013) Life in the 'charosphere' – does biochar in agricultural soil provide a significant habitat for microorganisms? Soil Biol Biochem 65:287–293
Rafiq MK, Bai Y, Aziz R, Rafiq MT, Mašek O, Bachmann RT, Joseph S, Shahbaz M, Qayyum A, Shang Z, Danaee M, Long R (2020) Biochar amendment improves alpine meadows growth and soil health in Tibetan plateau over a three year period. Sci Total Environ 717:135296
Rakitin AL, Kulichevskaya IS, Beletsky AV, Mardanov AV, Dedysh SN, Ravin NV (2024) *Verrucomicrobia* of the family *Chthoniobacteraceae* participate in xylan degradation in boreal peat soils. Microorganisms 12:2271
Rath KM, Murphy DN, Rousk J (2019) The microbial community size, structure, and process rates along natural gradients of soil salinity. Soil Biol Biochem 138:107607
Ren X, Wang F, Zhang P, Guo J, Sun H (2018) Aging effect of minerals on biochar properties and sorption capacities for atrazine and phenanthrene. Chemosphere 206:51–58
Ruamps LS, Nunan N, Chenu C (2011) Microbial biogeography at the soil pore scale. Soil Biol Biochem 43:280–286
Shade A, Jones Stuart E, Caporaso JG, Handelsman J, Knight R, Fierer N, Gilbert Jack A (2014) Conditionally rare taxa disproportionately contribute to temporal changes in microbial diversity. Mbio 5:e01371-14
Silber A, Levkovitch I, Graber ER (2010) pH-dependent mineral release and surface properties of cornstraw biochar: agronomic implications. Environ Sci Technol 44:9318–9323
Spokas KA (2010) Review of the stability of biochar in soils: predictability of O:C molar ratios. Carbon Manag 1:289–303
Spokas KA, Novak JM, Masiello CA, Johnson MG, Colosky EC, Ippolito JA, Trigo C (2014) Physical disintegration of biochar: an overlooked process. Environ Sci Technol Lett 1:326–332
Sun X, Zhang C, Liu K, Xu M, Cai A (2025) Long-term manure application enhances carbon use efficiency in soil aggregates by regulating microbial communities in cropland. Soil Biol Biochem 210:109945
Tan L, Sun C, Wang Y, Wang T, Wu G-L, He H, Zheng J (2020) Changes in biochar properties in typical loess soil under a 5-year field experiment. J Soils Sediments 20:340–351
Tan X-Y, Liu X-J, Lu D-C, Ye Y-Q, Liu X-Y, Yu F, Yang H, Li F, Du Z-J, Ye M-Q (2025) Insights into the physiological and metabolic features of *Thalassobacterium*, a novel genus of *Verrucomicrobiota* with the potential to drive the carbon cycle. Mbio 16:e00305-00325
Tang C, Yang J, Zhang L, Xie W, Yao R, Wang X, Wang R, Li T (2025) Abiotic and biotic factors mediate the decomposition of crop straw in saline farmland soils. Geoderma 459:117390

Trozzo L, D'Ottavio P, Kishimoto-Mo AW, Francioni M (2025) Wood gasification biochar enhances soil carbon sequestration without affecting greenhouse gas fluxes or wheat yield in sub-alkaline soil. Soil Tillage Res 251:106556
Wang L, O'Connor D, Rinklebe J, Ok YS, Tsang DCW, Shen Z, Hou D (2020) Biochar aging: mechanisms, physicochemical changes, assessment, and implications for field applications. Environ Sci Technol 54:14797–14814
Wang Y, Lin Q, Liu Z, Liu K, Wang X, Shang J (2023) Salt-affected marginal lands: a solution for biochar production. Biochar 5:21
Wang X, Riaz M, Babar S, Eldesouki Z, Liu B, Xia H, Li Y, Wang J, Xia X, Jiang C (2024) Alterations in the composition and metabolite profiles of the saline-alkali soil microbial community through biochar application. J Environ Manage 352:120033
Wang B, Shang C, Xie H, Sun H, Zhang Q, Xue L, Tack FMG, Hou D, Feng Y, Rinklebe J (2022) Unraveling natural aging-induced properties change of sludge-derived hydrochar and enhanced cadmium sorption site heterogeneity. Biochar 4:34
Wang X, Xia X, Riaz M, Babar S, El-Desouki Z, Qasim M, Wang J, Jiang C (2025) Biochar amendment modulate microbial community assembly to mitigate saline-alkaline stress across soil depths. J Environ Manage 385:125574
Wang D, Zhi C, Hu X, Wu Z, Song W, Wang J, Huang X, Yang F, Jiao Y, Li Y (2026) Impact of salinity gradient on sediment microbial communities and the functions of carbon, nitrogen, and sulfur cycling in coastal zone. Appl Geochem 196:106609
Z. Wang, S. Zhu, R. YU. 1993. Saline Soil in China, Science Publishing House.
Watzinger A, Feichtmair S, Kitzler B, Zehetner F, Kloss S, Wimmer B, Zechmeister-Boltenstern S, Soja G (2014) Soil microbial communities responded to biochar application in temperate soils and slowly metabolized C-labelled biochar as revealed by C PLFA analyses: results from a short-term incubation and pot experiment. Eur J Soil Sci 65:40–51
Xie W, Chen Q, Wu L, Yang H, Xu J, Zhang Y (2020) Coastal saline soil aggregate formation and salt distribution are affected by straw and nitrogen application: a 4-year field study. Soil Tillage Res 198:104535
Xu X, Kan Y, Zhao L, Cao X (2016) Chemical transformation of CO_2 during its capture by waste biomass derived biochars. Environ Pollut 213:533–540
Xu Z, Xu X, Tsang DCW, Cao X (2018) Contrasting impacts of pre- and post-application aging of biochar on the immobilization of Cd in contaminated soils. Environ Pollut 242:1362–1370
Yang F, Zhao L, Gao B, Xu X, Cao X (2016) The interfacial behavior between biochar and soil minerals and its effect on biochar stability. Environ Sci Technol 50:2264–2271
Yang C, Wang X, Miao F, Li Z, Tang W, Sun J (2020) Assessing the effect of soil salinization on soil microbial respiration and diversities under incubation conditions. Appl Soil Ecol 155:103671
Yang F, Xu Z, Huang Y, Tsang DCW, Ok YS, Zhao L, Qiu H, Xu X, Cao X (2021) Stabilization of dissolvable biochar by soil minerals: release reduction and organo-mineral complexes formation. J Hazard Mater 412:125213
Yang X, Wang L, Guo J, Wang H, Mašek O, Wang H, Bolan NS, Alessi DS, Hou D (2022) Aging features of metal(loid)s in biochar-amended soil: effects of biochar type and aging method. Sci Total Environ 815:152922
Yang H, Chen N, Wang Z, Liu J, Qin J, Zhu K, Jia H (2023) Biochar-associated free radicals reduce soil bacterial diversity: new insight into ecoenzymatic stoichiometry. Environ Sci Technol 57:20238–20248
Yang L, Peng Y, Wang S, Rong C, Dong H, Li H, Ge B (2025) Soil bacterial community composition but not alpha diversity altered along a gradient of Spartina alterniflora invasion on the coast of Yellow Sea, China. Front Mar Sci 12:1531902
Yi Q, Liang B, Nan Q, Wang H, Zhang W, Wu W (2020) Temporal physicochemical changes and transformation of biochar in a rice paddy: insights from a 9-year field experiment. Sci Total Environ 721:137670
Yin Y, Li M, Tao X, Yang C, Zhang W, Li H, Zheng Y, Wang X, Chen R (2023) Biochar enhanced organic matter transformation during pig manure composting: roles of the cellulase activity and fungal community. J Environ Manage 333:117464
Zhang G, Guo X, Zhu Y, Liu X, Han Z, Sun K, Ji L, He Q, Han L (2018) The effects of different biochars on microbial quantity, microbial community shift, enzyme activity, and biodegradation of polycyclic aromatic hydrocarbons in soil. Geoderma 328:100–108
Zhang P, Jiang Z, Wu X, Zhang N, Zhang J, Zou S, Wang J, Zang S (2024a) Effects of organic fertilizer and biochar on carbon release and microbial communities in saline–alkaline soil. Agronomy 14:1967
Zhang G, Bai J, Zhai Y, Jia J, Zhao Q, Wang W, Hu X (2024b) Microbial diversity and functions in saline soils: a review from a biogeochemical perspective. J Adv Res 59:129–140
Zhao R, Coles N, Wu J (2015) Carbon mineralization following additions of fresh and aged biochar to an infertile soil. CATENA 125:183–189
Zhao H, Tian X, Jiang Y, Zhao Y, Si B (2021) Effect of combining straw-derived materials and wood ash on alkaline soil carbon content and the microbial community. Eur J Soil Sci 72:1863–1878
Zhu H, Yang J, Yao R, Wang X, Xie W, Zhu W, Liu X, Cao Y, Tao J (2020) Interactive effects of soil amendments (biochar and gypsum) and salinity on ammonia volatilization in coastal saline soil. CATENA 190:104527
Zhu B, Li J, Li J, Chen X, Chi G (2025) Fungal community is more sensitive to the short-term application of biochar in saline farmland soil than bacterial community. Appl Soil Ecol 212:106219
Zimmerman AR (2010) Abiotic and microbial oxidation of laboratory-produced black carbon (Biochar). Environ Sci Technol 44:1295–1301